Forensic Toxicology (2020) 38:352–364
https://doi.org/10.1007/s11419-019-00521-x

ORIGINAL ARTICLE

Mass spectrometric characterization of carfentanil metabolism in human, dog, and rat lung microsomes via comparison to chemically synthesized metabolite standards

Li Kong[1] · Andrew J. Walz[1]

Received: 15 November 2019 / Accepted: 28 December 2019 / Published online: 21 January 2020

Abstract

Purpose The metabolism of carfentanil was assessed using human, dog, and rat pulmonary microsomes. Mass spectrometry based analysis allowed for metabolite identification and species differentiation. Participation of different metabolic enzymes in carfentanil biotransformation was also assessed.

Methods Metabolite profiling was accomplished by incubating 10 μM carfentanil in human, dog, and rat lung microsomes. The metabolites were separated and analyzed by ultra-high performance liquid chromatography/high-resolution mass spectrometry.

Results In total, 18 metabolites were detected. Nine metabolites were authentically identified through comparison to synthesized reference standards. In human lung microsomes, nine metabolites were identified. In dog lung microsomes, 15 metabolites were identified with three being dog specific. In rat lung microsomes, 15 metabolites were identified and two were rat specific. Proposed metabolic pathways included *N*-dealkylation, monohydroxylation, dihydroxylation, *N*-oxidation of piperidine ring nitrogen, and ketone formation. Participation of enzymes CYP2B6, CYP2E1, CYP2J2, and CYP3A4/5 to carfentanil metabolism was suggested by selective enzymatic inhibition.

Conclusions The pulmonary clearance in human lung microsomes was lower than the previously reported hepatic metabolism suggesting organ specific metabolic rates. The contribution of multiple cytochrome P450 enzymes to human, dog, and rat pulmonary microsomal carfentanil biotransformation varied between species. The identified metabolites may provide useful markers for possible forensic and clinical determination of the mode of ingestion but the use of dog and rat animal models was not indicated. To our knowledge, this is the first reported use of chemically synthesized reference standards for the unequivocal identification of lung carfentanil metabolites.

Keywords Carfentanil · Lung microsomes · Metabolite identification · Selective CYP enzyme inhibitor · Ultra-high performance liquid chromatography · High-resolution mass spectrometry

Introduction

Carfentanil is the most potent synthetic opioid with activity 10,000 times that of morphine and 20–30 times that of fentanyl [1–3]. It is approved for use in veterinary medicine to immobilize free-ranging or confined large animals [4, 5]. Pharmacological studies have been reported in not only animals but also in humans [5–10]. [^{11}C] labeled carfentanil has been applied, in human studies, to map brain μ-opioid receptors, investigate pain mechanisms, and examine opioid dependence [11–14]. Additionally, carfentanil and remifentanil were identified as possible components in an aerosol used by Russian security forces to resolve a terrorist theater siege in 2002 [15,

Electronic supplementary material The online version of this article (https://doi.org/10.1007/s11419-019-00521-x) contains supplementary material, which is available to authorized users.

✉ Li Kong
li.kong.civ@mail.mil

[1] Research and Technology Directorate, Combat Capabilities Development Command Chemical Biological Center, U. S. Army, Aberdeen Proving Ground, MD 21010-5424, USA

16]. That fact combined with the inhalation risk posed to law enforcement through illicit carfentanil production/distribution and the increased illicit use of carfentanil in humans [17–20] suggested that an examination of the biological transformation of carfentanil by lung tissue was merited.

The lung is a pharmacologically active organ which can absorb, retain, metabolize, and release many drugs and compounds [21, 22]. Not only may drugs undergo first-pass metabolism in the lung after inhalation but also following oral or intravenous administration since the lung is an efficient organ for extracting drugs from blood circulation [21, 23]. While lung metabolic rates are generally much slower than the intestinal-hepatic rates, the same metabolic enzymes (CYP2B, CYP2E, CYP2J, and CYP3A) are also expressed in the lung [21, 23–25]. These characteristics suggest that the lung plays an important role in systemic drug elimination and that lung tissue may produce unique drug metabolites [26]. While there is a report on the metabolism of carfentanil by human liver microsomes and hepatocyte [27], no studies on carfentanil lung metabolism have been published. Furthermore, studies suggest that species differences exist in the catalytic activities of cytochrome P450 enzymes [28]. An examination of these potential differences could aid in the development of animal models for human drug pharmacokinetics and potential metabolite toxicity.

High-resolution mass spectrometry (HRMS) has been employed as a reliable and powerful analytical technique for drug metabolism studies in terms of metabolites identification from biological matrices. Most drug metabolic studies rely upon putative annotation of metabolite structures due to the significant efforts required to confirm the proposed structures through chemical synthesis. To differentiate the potential isomers in this study, previously synthesized liver metabolites of carfentanil were employed as standards for definitive lung metabolite identification [29].

Furthermore, the ability of human, dog, and rat lung microsomes to metabolize carfentanil has been assessed and the structures of carfentanil metabolites have been proposed. A preliminary examination of the roles of specific cytochrome P450 enzymes in the metabolic pathway of carfentanil was also accomplished through the use of known cytochrome P450 chemical inhibitors. Cytochrome P450 enzymes to be examined were selected based on previously demonstrated expression in human lung [21, 25, 30]. Thus, CYP2B6, CYP2E1, CYP2J2, and CYP3A4/5 were considered to be the cytochrome P450 enzymes most likely to be active in the human pulmonary biotransformation of carfentanil. Moreover, the activity levels of isozymes were also analyzed in dog and rat lung microsomes in order to evaluate interspecies variations.

Materials and methods

Chemicals and reagents

Carfentanil citrate, carfentanil-d_5 citrate, metabolites M1, M7, M9, M10, M11, M13, M15, M17, and M18 were synthesized at Combat Capabilities Development Command Chemical Biological Center [29]. Ketoconazole, ticlopidine, telmisartan, diethyldithiocarbamate, NADPH (β-nicotinamide adenine dinucleotide 2′-phosphate reduced tetrasodium salt hydrate), magnesium chloride, ammonia formate, and formic acid were purchased from Sigma-Aldrich (St. Louis, MO, USA); OmniSolv® LC–MS acetonitrile and high purity water (B and J brand) from VWR International (Radnor, PA, USA); pooled mixed gender human, male beagle dog, and male IGS SD rat lung microsomes from Sekisui XenoTech, LLC (Kansas City, KS, USA) and stored at − 80 °C until use. All other agents were of highest grade available.

Incubation of carfentanil with pooled human, dog, and rat lung microsomes

Carfentanil (10 µM) was incubated in 200 µL of a reaction solution containing 0.1 M potassium phosphate buffer (pH 7.4), 3 mM $MgCl_2$, 2 mg/mL of human, dog, or rat lung microsomal protein. After 5 min at 37 °C, 2 mM NADPH was added to initiate the reaction. The reactions were performed in triplicate, and a control reaction, without lung microsomes, was performed in duplicate. Each reaction was run for 30, 60, 90, 120, and 180 min, and then quenched by the addition of an equal volume of ice-cold acetonitrile containing internal standard (1 µM carfentanil-d_5). The incubation mixtures were vortexed and then centrifuged at 2250×g for 10 min. The supernatants were frozen and stored at − 80 °C until analysis.

Chemical inhibition study was achieved by adding P450 inhibitors into the incubation mixtures containing carfentanil (10 µM) and lung microsomes of human, dog, and rat (2 mg/mL) system as described above for carfentanil biotransformation assay. The P450 inhibitors and concentrations were selected on the basis of previous reports and were as follows: CYP2B6 (ticlopidine, 50 µM) [31, 32], CYP2E1 (diethyldithiocarbamate, 50 µM) [33], CYP2J2 (telmisartan, 20 µM) [34], and CYP3A4/5 (ketoconazole, 3 µM) [35]. Reactions were initiated with NADPH after initial preincubation of microsomes with carfentanil and P450 inhibitor for 10 min at 37 °C. Inhibition experiments were conducted in triplicate with replicate incubations. Inhibition was measured and calculated as the percentage relative to control samples which had no inhibitors added.

Semiquantitative analysis of carfentanil and its metabolites was accomplished by calculating the relative peak areas of carfentanil and the resulting metabolites against that of the internal standard carfentanil-d_5 using full scan HRMS and the results are expressed as a percentage of the control.

Ultra-high performance liquid chromatography–high resolution mass specstrometry conditions

Ultra-high performance liquid chromatography–high-resolution mass spectrometry (UHPLC–HRMS) was performed on a Thermo Fisher Scientific Ultimate 3000 HPLC system coupled to an Orbitrap Fusion Tribrid mass spectrometer (Orbitrip Fusion TMS; Thermo Fisher Scientific, Waltham, MA, USA). Metabolite separation was achieved using a Kinetex® EVO C18 column (100 × 2.1 mm i.d., 1.7 µm particle size, 100 Å pore size; Phenomenex, Torrance, CA, USA) at a flow rate of 280 µL/min. Mobile phase A was 10 mM ammonium formate aqueous solution with 0.1% formic acid and mobile phase B was acetonitrile with 0.1% formic acid. The elution gradient was as follows: 0–1 min, an isocratic elution of 5% B; 1–10 min, a linear gradient to 40% B; 10–14 min, a linear gradient to 95% B; 14–15.7 min, an isocratic elution of 95% B; 15.8 min, a gradient back to 5% B. The total run time was 17 min. The injection volume was 5 µL. The autosampler chamber was maintained at 4 °C with a column temperature at 30 °C.

Heated electrospray ionization (HESI) was utilized in the positive ion mode, and carfentanil and its metabolites were analyzed from *m/z* 100 to 800. Orbitrap Fusion TMS had two fragmentation techniques, collision induced dissociation (CID) and higher-energy collisional dissociation (HCD). In this study, HCD was used as the fragmentation technique. The parameters used for the mass spectrometer were as follows: spray voltage, 4100 V; sheath gas flow rate, 40 respective arbitrary units; auxiliary gas flow rate, 20 respective arbitrary units; ion transfer tube temperature, 325 °C; vaporizer temperature, 300 °C; MS^1 detector, Orbitrap; MS^1 resolution, 120,000; MS^1 scan range, 100–800; MS^1 maximum injection time, 100 ms; MS^1 automated gain control (AGC) target, 100,000; S-lens radio frequency level, 60 V; MS^2 HCD collision energy, 30%; MS^2 detector, Orbitrap; MS^2 resolution, 60,000; MS^2 AGC target, 50,000; MS^2 maximum injection time, 35 ms; MS^2 start mass, 50. In all experiments active internal mass calibration was employed during the analysis. *Xcalibur* Qual and Quan Browser software (Thermo Fisher Scientific) were used for the qualitative and semiquantitative analysis.

Results

Biotransformation of carfentanil by human, dog, or rat lung microsomes

Metabolism of carfentanil in human, dog, and rat lung microsomes resulted in 9, 15, and 15 metabolites, respectively (Fig. 1). Metabolites were not observed in control samples indicating that metabolite formation was enzyme-dependent. The HRMS provided the accurate molecular weights of carfentanil metabolites, and the molecular formulae could be deduced. Proposed structural information was elucidated through analysis of the product ion scans using MS/MS. Table 1 lists the following information: all metabolites with proposed biotransformation, UHPLC retention times, microsomal source, elemental composition of protonated molecules, measured mass, and mass error. Metabolites were labeled "M" followed by a number referencing the order of elution. The structures of metabolites M1, M7, M9, M10, M11, M13, M15, M17, and M18 were confirmed using synthetic reference standards.

Product ion formation of carfentanil

Prior to characterizing the metabolites, the mass characteristics of carfentanil were investigated. In the positive ion mode, carfentanil formed a protonated molecule $[M+H]^+$ at *m/z* 395.23353, which yielded characteristic product ions *at m/z* 105.06991, 113.05975, 134.09642, 146.09644, 186.12768, 202.12262, 246.14873, 279.18538, and 335.21156, as shown in Fig. 2. The base peak at *m/z* 335.21156 was formed by the loss of a carbomethoxy. Product ion at *m/z* 279.18538 was generated by loss of both the carbomethoxy group and propanone. The ion at *m/z* 246.14873 resulted from loss of the *N*-phenyl-propionamide.

Metabolite identification

Norcarfentanil (M1)

M1 eluted at 8.28 min with an accurate protonated molecule $[M+H]^+$ at *m/z* 291.17015. *N*-Dealkylation was demonstrated by the complete loss of the phenethyl substructure indicated by the absence of *m/z* 105.06991, 134.09642, and 186.12768 (Figs. 2, 3). M1 was confirmed by reference standard (Fig. 3).

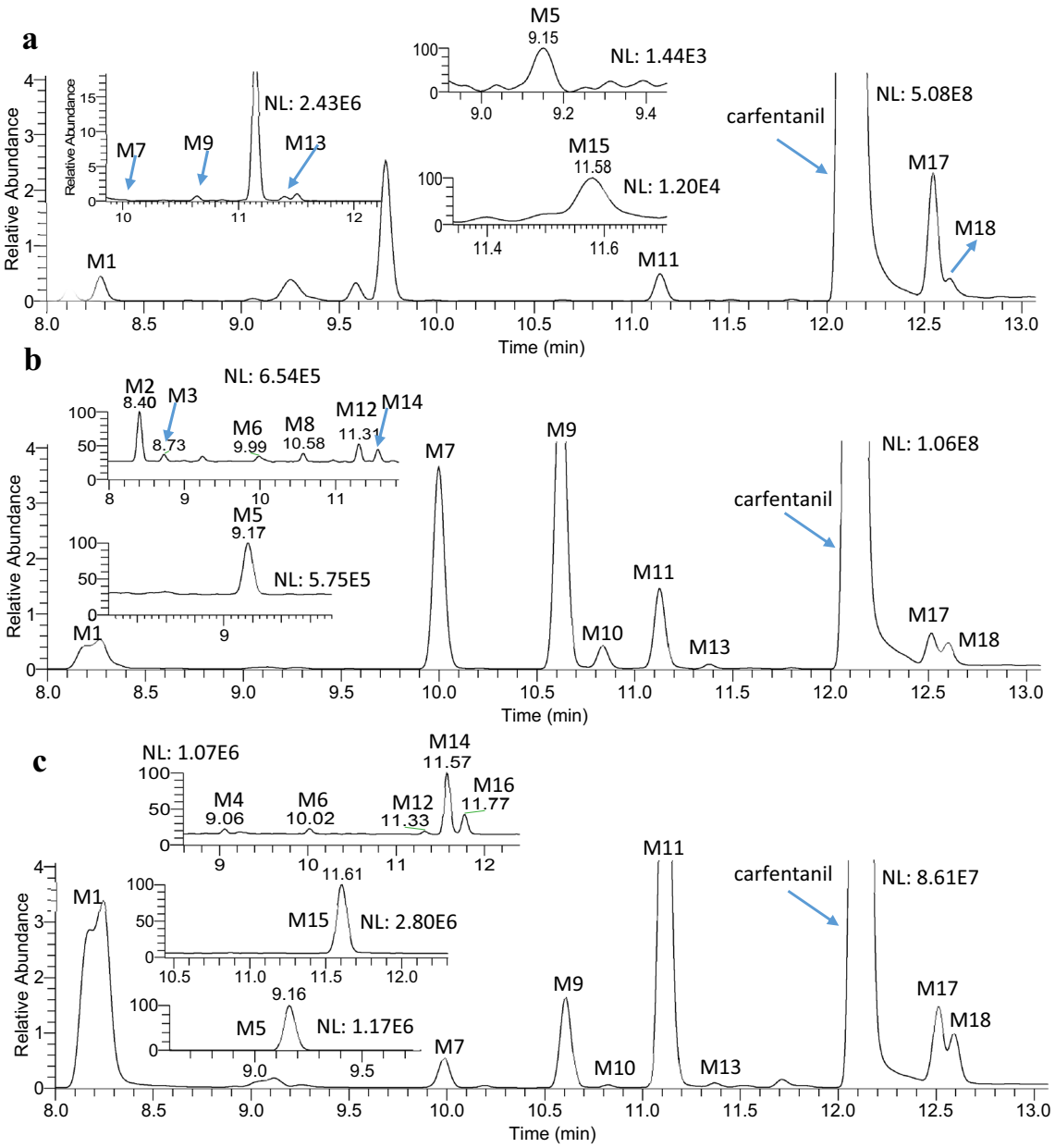

Fig. 1 Combined extracted ion chromatograms of carfentanil and metabolites in **a** human, **b** dog, and **c** rat lung microsomes. *NL* normalized level

Monohydroxylated metabolites M7, M9, M10, M11, and M13

M7, M9, M10, M11, and M13 were generated by monohydroxylation. M7 was formed by hydroxylation at the *N*-propanoic group based on the presence of *m/z* 218.11749 and the preservation of the phenethyl (*m/z* 105.06989, 134.09643), piperidine (*m/z* 186.12764), and *N*-phenyl (*m/z* 158.09641) containing product ions. M7 was confirmed by reference standard (Suppl. Fig. S1). M9, M10, M11, and M13 were hydroxylated at the phenethyl moiety based on product ions at *m/z* 121.06478, 150.09128, and 162.09132. These product ions incorporate the phenethyl containing precursor fragments at *m/z* 105.06991, 134.09642, and 146.09644 with an additional oxygen atom. Separation of the ortho (M13), meta (M10), and para (M9) isomers was accomplished and the structures were confirmed by reference standards (Suppl. Fig. S1). The hydroxylation of M11 occurred on the phenethyl-linker which was also confirmed by reference standard (Suppl. Fig. S1).

Table 1 Elemental compositions, measured masses, and mass errors of carfentanil and its metabolites identified in human, dog, and rat lung microsomes

Precursor & Metabolites	Biotransformation	RT (min)	Lung microsomes	Elemental composition of molecular ion $[M+H]^+$	Precursor ion (m/z)	Mass error (ppm)	Diagnostic product ions *(m/z)*
Carfentanil		12.18		$C_{24}H_{31}N_2O_3^+$	395.23353	− 1.54	105.06991, 113.05975, 134.09642, 146.09644, 186.12768, 202.12262, 246.14873, 279.18538, 335.21158
M1	*N*-Dealkylation of piperidine ring	8.28	Human, dog, rat	$C_{16}H_{23}N_2O_3^+$	291.17015	0.58	110.06011, 113.05975, 142.08627, 146.09640, 158.09641, 175.12296, 231.14911, 259.14399
M2	Dihydroxylation	8.40	Dog	$C_{24}H_{31}N_2O_5^+$	427.22260	0.35	113.05975, 121.06481, 142.08627, 150.09135, 202.12262, 218.11753, 262.14362, 295.18027, 367.20131
M3	Dihydroxylation	8.73	Dog	$C_{24}H_{31}N_2O_5^+$	427.22260	0.35	113.05975, 150.09130, 218.11750, 262.14362, 295.18030, 367.20139
M4	Dihydroxylation	9.06	Rat	$C_{24}H_{31}N_2O_5^+$	427.22254	0.49	113.05975, 132.08077, 162.09130, 232.13314, 262.14364, 295.18040, 367.20140
M5	Ester hydrolysis + hydroxylation of propanoic group	9.17	Human, dog, rat	$C_{23}H_{29}N_2O_4^+$	397.21196	0.55	105.06988, 134.09642, 188.14338, 232.13311, 279.18538, 325.19080, 351.20648
M6	Dihydroxylation	10.02	Dog, rat	$C_{24}H_{31}N_2O_5^+$	427.22260	0.35	113.05971, 148.07565, 178.08623, 248.12805, 260.12801, 278.13855, 367.20137
M7	Monohydroxylation	10.04	Human, dog, rat	$C_{24}H_{31}N_2O_4^+$	411.22818	− 0.85	105.06989, 113.05975, 134.09643, 158.09641, 186.12764, 218.11749, 246.14868, 279.18539, 351.20645
M8	Hydroxylation + *N*-oxidation	10.58	Dog	$C_{24}H_{31}N_2O_5^+$	427.22249	0.61	105.06992, 113.05964, 150.09132, 247.14404, 290.13858, 319.16505

Table 1 (continued)

Precursor & Metabolites	Biotransformation	RT (min)	Lung microsomes	Elemental composition of molecular ion $[M+H]^+$	Precursor ion (m/z)	Mass error (ppm)	Diagnostic product ions *(m/z)*
M9	Monohydroxylation	10.66	Human, dog, rat	$C_{24}H_{31}N_2O_4^+$	411.22831	− 1.17	113.05979, 121.06486, 150.09134, 202.12262, 262.14348, 295.18003, 351.20601
M10	Monohydroxylation	10.86	Dog, rat	$C_{24}H_{31}N_2O_4^+$	411.22763	0.49	113.05974, 146.09638, 150.09131, 162.09130, 202.12256, 262.14361, 295.18028, 351.20643
M11	Monohydroxylation	11.16	Human, dog, rat	$C_{24}H_{31}N_2O_4^+$	411.22764	0.46	113.05973, 132.08077, 150.09131, 162.09129, 202.12250, 232.13308, 262.14357, 295.18023, 351.20637, 379.20146
M12	Hydroxylation + *N*-oxidation	11.31	Dog, rat	$C_{24}H_{31}N_2O_5^+$	427.22254	0.49	121.06483, 158.08114, 202.12264, 247.14400, 274.14364, 303.17012
M13	Monohydroxylation	11.41	Human, dog, rat	$C_{24}H_{31}N_2O_4^+$	411.22762	0.51	113.05970, 121.06476, 150.09126, 162.09124, 202.12255, 262.14347, 295.18007, 351.20618, 379.20117
M14	Hydroxylation + *N*-oxidation	11.56	Dog, rat	$C_{24}H_{31}N_2O_5^+$	427.22248	0.63	113.05975, 148.07565, 202.12268, 247.14403, 274.14365, 303.17013
M15	Ketone formation on phenethyl linker	11.60	Human, rat	$C_{24}H_{29}N_2O_4^+$	409.21201	0.42	113.05975, 132.08077, 150.09131, 162.09129, 202.12250, 232.13308, 244.13306, 262.14357, 295.18023, 351.20637
M16	Hydroxylation + *N*-oxidation	11.77	Rat	$C_{24}H_{31}N_2O_5^+$	427.22253	0.51	113.05974, 132.08079, 158.08115, 202.12256, 260.12800, 274.14366, 303.17012
M17	*N*-Oxidation of piperidine N (*trans*)	12.56	Human, dog, rat	$C_{24}H_{31}N_2O_4^+$	411.22769	0.34	105.06993, 132.08076, 150.09131, 202.12164, 230.11750, 244.13328, 247.14396, 262.14357, 274.14361, 303.17007, 355.20141

Table 1 (continued)

Precursor & Metabolites	Biotransformation	RT (min)	Lung microsomes	Elemental composition of molecular ion $[M+H]^+$	Precursor ion (m/z)	Mass error (ppm)	Diagnostic product ions *(m/z)*
M18	*N*-Oxidation of piperidine N (*cis*)	12.68	Human, dog, rat	$C_{24}H_{31}N_2O_4^+$	411.22763	0.49	105.06993, 134.09643, 150.09131, 202.12221, 230.11746, 244.13426, 262.14361, 274.14363, 303.17010, 335.21198, 379.20138
M1[a] (norcarfentanil)		8.33		$C_{16}H_{23}N_2O_3^+$	291.17015	0.58	110.06012, 113.05976, 142.08627, 146.09642, 158.09638, 175.12293, 231.14906
M7[a]		10.05		$C_{24}H_{31}N_2O_4^+$	411.22837	− 1.31	105.06991, 113.05974, 134.09643, 158.09641, 186.12758, 218.11750, 246.14872, 279.18539, 351.20642
M9[a]		10.66		$C_{24}H_{31}N_2O_4^+$	411.22836	− 1.29	113.05970, 121.06478, 150.09127, 202.12254, 262.14353, 295.18016, 351.20627
M10[a]		10.86		$C_{24}H_{31}N_2O_4^+$	411.22831	− 1.17	113.05983, 146.09657, 150.09142, 162.09142, 202.12273, 262.14365, 295.18022, 351.20629
M11[a]		11.16		$C_{24}H_{31}N_2O_4^+$	411.22830	− 1.14	113.05973, 132.08076, 150.09131, 162.09128, 202.12256,232.13308, 262.14356, 295.18017, 351.20633, 379.20125
M13[a]		11.41		$C_{24}H_{31}N_2O_4^+$	411.22828	− 1.09	113.05972, 121.06482, 150.09132, 162.09132, 202.12265, 262.14362, 295.18041, 351.20647, 379.20146
M15[a]		11.60		$C_{24}H_{29}N_2O_4^+$	409.21407	− 4.62	113.05984, 132.08076, 150.09131, 162.09128, 202.12273, 232.13308, 244.13303, 262.14356, 295.18017, 351.20633

Table 1 (continued)

Precursor & Metabolites	Biotransformation	RT (min)	Lung microsomes	Elemental composition of molecular ion $[M+H]^+$	Precursor ion (m/z)	Mass error (ppm)	Diagnostic product ions (*m/z*)
M17[a]		12.56		$C_{24}H_{31}N_2O_4^+$	411.22836	− 1.29	105.06991, 132.08074, 150.09129, 202.12257, 230.11742, 244.13304, 247.14391, 262.14352, 274.14353, 303.16998, 355.20128
M18[a]		12.68		$C_{24}H_{31}N_2O_4^+$	411.22829	− 1.12	105.06990, 134.09638, 150.09127, 202.12255, 230.11736, 244.13301, 262.14352, 274.14353, 303.16998, 335.21145, 379.20118

RT retention time

[a]Reference standard

N-Oxidation metabolites M17 and M18

M17 and M18, with accurate protonated molecules $[M+H]^+$ at *m/z* 411.22769 and 411.22763, were eluted after the parent at 12.56 and 12.68 min (Fig. 1) which was a consistent elution pattern for *N*-oxides [36]. M17 and M18 (Suppl. Fig. S2) were identified as *trans*- and *cis*-diastereoisomeric *N*-oxides of the piperidine nitrogen as indicated by product ions at *m/z* 230.11750, 262.14357, and 303.17007. Product ions at *m/z* 105.06993 and 274.14361 indicated an unmodified phenethyl moiety and unchanged *N*-propanoic moiety, respectively. The ions at *m/z* 262.14357 indicated the *N*-oxide product of parent product ion at *m/z* 246.14873 (Fig. 2). Both M17 and M18 were confirmed by reference standards (Suppl. Fig. S2).

Other metabolites

Eight secondary metabolites M2, M3, M4, M6, M8, M12, M14, and M16 were generated by either an additional hydroxylation or an additional *N*-oxidation. M2 [retention time (RT): 8.40 min], M3 (RT 8.73 min), and M4 (RT 9.06 min) possibly resulted from further hydroxylation of M7 on the phenethyl group or further hydroxylation of M9, M10, M11, or M13 on the *N*-propanoic moiety indicated by the same characteristic ions of *m/z* 262, 295, and 367 (*m/z* 351 + 16) (Suppl. Fig. S3).

The fragment ions at *m/z* 166.08618 (134 + 32), 178.08623 (146 + 32), and 248.12812 of M6 indicated dihydroxylation of the phenethyl group, while ions at *m/z* 278.13855, 311.17537, and 367.20137 indicated a second hydroxylation of the characteristic ions at *m/z* 262, 295, and 351 of M9, M10, M11, or M13.

Metabolite M8 had a characteristic ion at *m/z* 105.06992 which indicated an unmodified phenethyl moiety. However, product ions at *m/z* 290.13858 and 319.16505 could result from *N*-oxidation (diagnostic ions at *m/z* 274 and 303 with a mass shift of hydroxylation). Since hydroxylation on the phenethyl moiety was ruled out, the hydroxylation was proposed on the *N*-propanoic moiety.

Metabolites M12, M14, and M16 shared the same diagnostic ions for *N*-oxidation at *m/z* 274 and 303. Because the hydroxylation of M8 was proposed on *N*-propanoic moiety, the second hydroxylations of metabolites M12, M14, and M16 were proposed on the phenethyl moiety (Suppl. Fig. S3).

M5 (*m/z* 397.21218, RT 9.17 min) may be produced by ester hydrolysis of M7, based on the mass shift of 14.01622, corresponding to methyl group loss. The presence of product ion at *m/z* 232.13311 (Suppl. Fig. S4) indicated ester hydrolysis of the precursor ion at *m/z* 246.14848 of M7 (Suppl. Fig. S1).

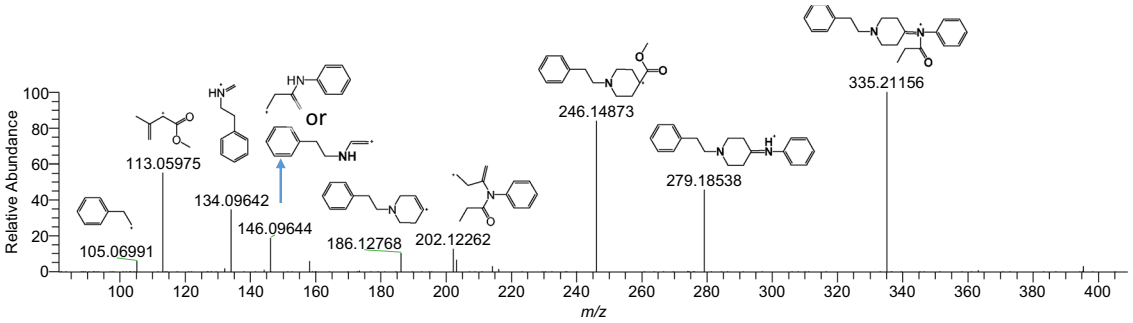

Fig. 2 MS/MS spectrum of carfentanil and identified product ion structures

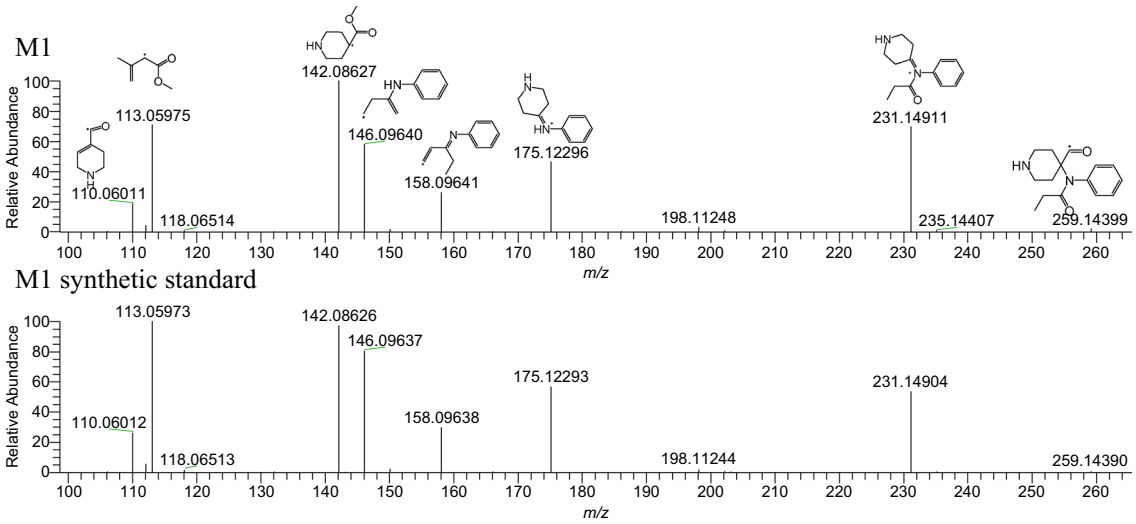

Fig. 3 MS/MS spectrum of M1 and identified product ion structures

M15 (*m/z* 409.21201, RT 11.60 min) was the only ketone metabolite identified and was confirmed by synthesized reference standard. Suppl. Fig. S5 and Table 1 shows the identified fragmentation ions and it is proposed to be the dehydrogenation product from metabolite M11 (Fig. 4).

Metabolic pathways and interspecies comparison

In the presence of NADPH, when carfentanil was incubated with lung microsomes of human, dog, and rat for up to 3 h, there were 9.4, 15.9, 21.7% loss of carfentanil (Fig. 5), respectively, indicating that carfentanil was metabolically less active in lung microsomes than in liver microsomes. The incubation resulted in 18 metabolites being detected. M1, M7, M9, M10, M11, M13, M15, M17, and M18 were confirmed by comparison with reference standards. All other proposed structures are tentative and need further verification. Based on the identified metabolites, the metabolic pathways are proposed as seen in Fig. 4. The predominant metabolic pathways of carfentanil in lung microsomes involved *N*-dealkylation, ester hydrolysis, hydroxylation, dihydroxylation, *N*-oxidation, and ketone formation. M17, M9, and M11 were identified as the primary metabolites in human, dog, and rat lung microsomes, respectively (Fig. 5). In human lung microsomes, the three major metabolic pathways were *N*-oxidation of piperidine, *N*-dealkylation, and hydroxylation on the phenethyl-linker, respectively. These three major pathways resulted in the formation of the three most abundant metabolite M17, M1, and M11 and accounted for 0.96, 0.39, and 0.29% of initial amount of carfentanil (Fig. 5). Therefore, both M17 and M11 could be used as biomarkers for the detecting of the illicit use of carfentanil in humans. In dog and rat, hydroxylation at the phenethyl moiety was the major pathway. Metabolites M9 and M11 were predominant metabolites in dog and rat lung microsomes, and accounted for 4.85 and 6.03% of initial amount of carfentanil, respectively (Fig. 5).

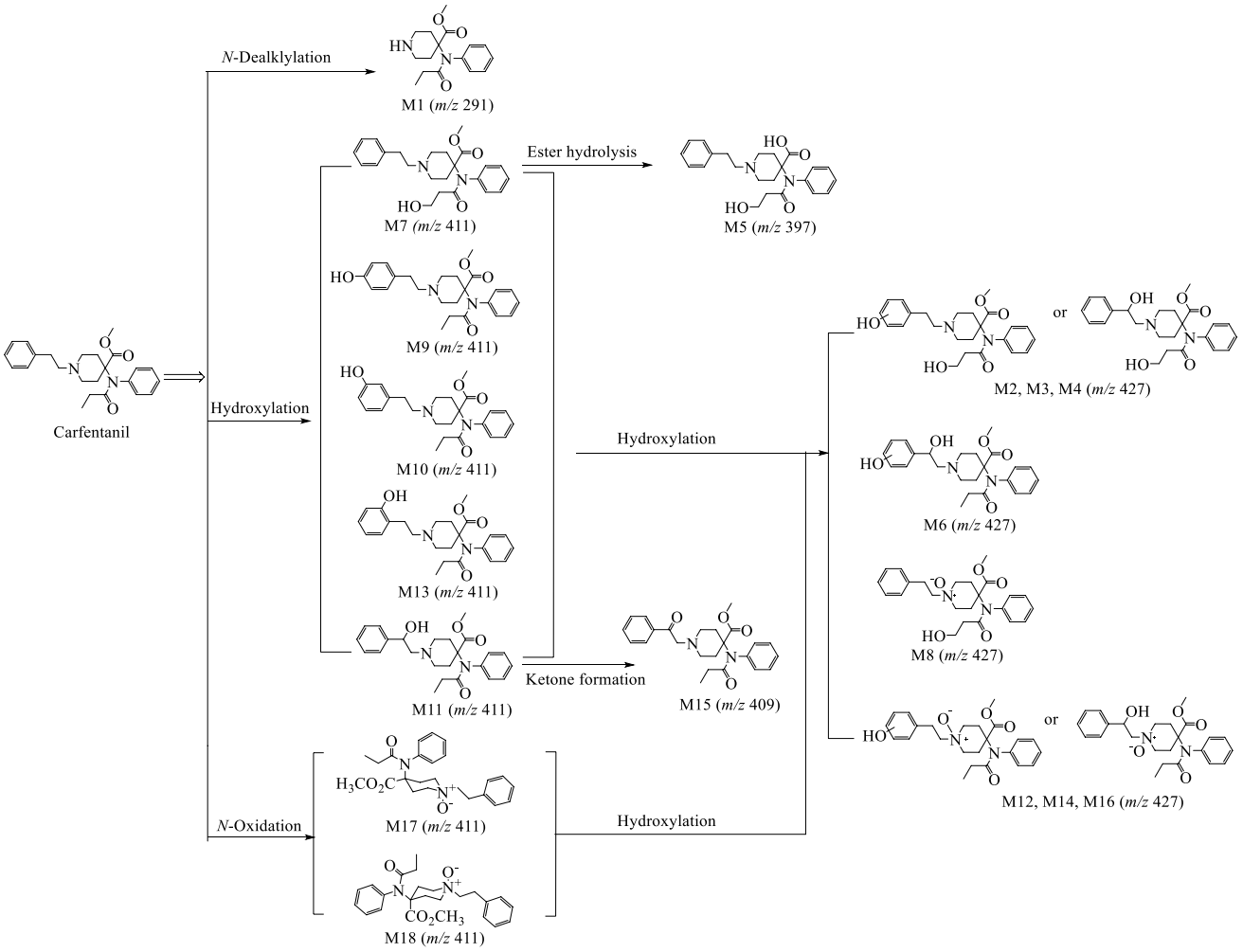

Fig. 4 Proposed metabolic pathways of carfentanil in human, dog, and rat lung microsomes

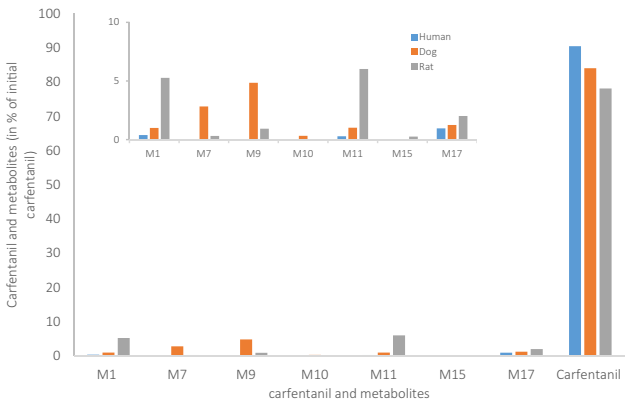

Fig. 5 Percentages of metabolism of carfentanil after 3 h incubation with human, dog, and rat lung microsomes. Each bar represents the mean of triplicate determinations (< 15% variance)

Table 2 Inhibition percentages of carfentanil metabolism during the lung microsomal incubation in the presence of specific CYP enzyme inhibitors

Inhibitor	% Inhibition of metabolism			Inhibitory spectrum
	Human	Dog	Rat	
None	0	0	0	
Ticlopidine (50 μM)	46.3	35.0	39.7	CYP2B6
Diethyldithiocarbamate (50 μM)	33.6	30.6	36.4	CYP2E1
Telmisartan (20 μM)	28.2	30.8	52.1	CYP2J2
Ketoconazole (3 μM)	14.8	39.7	65.0	CYP3A4/5

Cytochrome P450 enzyme inhibition assays

To assess the involvement of the major constitutive CYP enzymes in the metabolism of carfentanil, ticlopidine,

diethyldithiocarbamate, telmisartan, and ketoconazole were used as selective inhibitors. As shown in Table 2, the approximate percent inhibition by ticlopidine (specific for CYP2B6), diethyldithiocarbamate (specific for CYP2E1), telmisartan (specific for CYP2J2), and ketoconazole (specific for CYP3A4/5) was as follows: 46, 34, 28, and 15% in human lung microsomes; 35, 31, 31, and 40% in dog lung microsomes; and 40, 36, 52, and 65% in rat lung microsomes, respectively. The involvement of other CYP enzymes was not considered because they were not detected or had no reported metabolic activity in human lung tissue [21]. Furthermore, CYP1A1 was not considered because it has only been expressed in the lung tissue of smokers [21, 23]. The data demonstrated varied levels of inhibition in the three species examined. Even with the relatively slow rate of carfentanil metabolism in human, dog, and rat lung microsomes, enzyme-specific contributions were seen. Feasel et al. [27] reported that carfentanil is rapidly metabolized in human liver microsomes with CYP3A4 as the likely predominant metabolic enzyme. Chemical inhibition in this work indicated the likely involvement of CYP3A4/5 and also the involvement of 2B6, 2E1, and 2J2 in the metabolism of carfentanil in lung microsomes of human, dog, and rat. The human lung microsome inhibition data suggested a major role for CYP2B6 with a lesser role for CYP3A4/5. However, the addition of ketoconazole resulted in 40% and 65% inhibition of carfentanil metabolism in dog and rat lung microsomes indicated that CYP3A4/5 mediated metabolism were more dominant in dog and rat. These results further indicate that these animals would not be appropriate to serve as the surrogate human model for the evaluation of the potential drug–drug interactions in vivo.

Discussion

Investigation of carfentanil metabolism in human liver microsomes and hepatocytes resulted in 12 identified metabolites with norcarfentanil and hydroxylation of piperidine ring as the two most abundant metabolites [27]. Feasel et al. [27] suggested that the rapid clearance in human liver microsomes (HLM), but much slower one in hepatocytes could be due to a larger volume of distribution and plasma protein binding.

Compared with metabolism in HLM and hepatocytes [27], the loss of carfentanil as a function of time suggested that carfentanil was transformed more slowly in lung microsomes of human, dog, and rat, but comparable to the reported metabolic rate in human hepatocytes. Metabolites M1, M7, M9, M12, M14, M15, M16, M17, and M18 were detected in human hepatocytes [27] and in this study. Metabolites M2, M3, M4, M5, M6, M8, M10, and M13 were newly identified metabolites, which were not observed in the liver microsomes. Furthermore, previously reported liver metabolites including piperidine ring monohydroxyaltion and phase II glucuronidation were not detected in any of the examined lung microsomes and the lung S9 fraction (data not shown) from the same three species. These results demonstrate that variation exist between liver and lung metabolic rate and also in the metabolic profile.

The aim of a preclinical metabolic study is to provide background data for the possible employment of animals for toxicological experiments. Species dependent metabolic difference have been frequently observed, which complicates cross-species extrapolation to predict the human pharmacokinetics of drugs and to assess risk for drug-drug interaction [28, 37]. In the current study, rat lung microsomes showed the fastest metabolism (Fig. 5) and their high extrahepatic clearance resulted in 15 metabolites being detected (Table 1). M11 was the most abundant metabolite and M4 and M16 were rat-specific. In dog lung microsomes, carfentanil showed moderate metabolism which led a total of 15 metabolites being detected. Among them, M2, M3, and M8 were specifically found in dog (Table 1). In human lung microsomes, carfentanil showed slowest metabolism and nine metabolites were detected. The data indicate that significant differences exist among the dog, rat, and human lung metabolic profile, thus prohibiting the use of dog or rat as animal model to predict human pharmacokinetic behavior of carfentanil.

The relative contributions of individual P450 enzymes to the biotransformation of carfentanil in human, dog, and rat lung microsomes were studied using selective P450 chemical inhibitors (Table 2). The present study clearly established that several CYP450 isozymes contribute to carfentanil biotransformation in human, dog, and rat lung microsomes, and the relative contributions of these enzymes vary among species based on the specific inhibition of carfentanil metabolism by selective CYP450 inhibitors. As opposed to the predominant role of CYP3A4 in carfentanil hepatic metabolism [27], CYP2B6 appears to play a significant role in carfentanil metabolism in human lung. Other CYP450 isozymes, including CYP 2E1, 2J2, and 3A4/5, appear to play minor roles. These observations indicated the presence of tissue specific differences between human lung microsomal and liver microsomal carfentanil metabolic profiles.

It should be noted that the μ-opioid receptor (MOR) activity of synthesized carfentanil and it primary metabolites from human liver microsomes has been reported by our group very recently [29]. The EC_{50} values (nM) of the parent compound and some of the metabolites were as follows: carfentanil (0.0049), M1 (17), M7 (0.28), M9 (0.028), M10 (0.014), M11 (0.0051), M13 (0.0024), M15 (0.20), and M17/M18 (4.4). The MOR activity of M11 was nearly identical to the parent carfentanil, while M13, which was detected in the human lung but not in the liver metabolic studies, was twice

as active as the parent compound. While high protein binding and a larger volume of distribution might contribute to the longer half-life of carfentanil in hepatocytes, its duration of action may be enhanced by the active metabolites (M11 and M13). These active metabolites may also contribute to enhancing the toxicity of carfentanil.

Conclusions

The increased illicit use of carfentanil in humans [17–20] has heightened the need for more detailed characterization of its metabolic biotransformation. The metabolic profiles of carfentanil in human, dog, and rat lung microsomes were investigated and the metabolites were identified by UHPLC-Orbitrap Fusion MS using chemically synthesized reference standards. A total of 18 metabolites were detected with 8 being newly identified. In addition, we could successfully separated the three *ortho*-, *meta*-, and *para*-hydroxylated isomers and also a *trans*- and *cis*-diastereoisomeric *N*-oxide pair of metabolites. M17 was the most abundant metabolite in human lung microsomes. M9 was the most abundant in dog and M2, M3, and M8 were specifically detected in dog lung microsomes. M11 was the most abundant metabolite in rat and M4 and M16 were rat-specific.

Even though norcarfentanil (M1), one of the three major metabolites, is a good indicator to carfentanil exposure, but is not exclusive to carfentanil, e.g., remifentanil shared the same metabolite. Containing the entire carfentanil structure, metabolite M17, *N*-oxide of the piperidine nitrogen, and M11, hydroxylation on phenethyl-linker, were the other two most abundant metabolites of carfentanil in human lung microsomes, and thus could serve as forensic biomarkers of carfentanil. This study provides valuable information on the in vitro biotransformation of carfentanil and the identified metabolites data will aid clinical laboratories in targeting additional markers of carfentanil intake.

Acknowledgements This work was funded by the Defense Threat Reduction Agency (DTRA) under Project number CB3662.

Compliance with ethical standards

Conflict of interest The authors declare that they have no conflict of interest.

Ethical approval This article does not contain any studies with human participants or animals performed by any of the authors.

References

1. Lust EB, Barthold C, Malesker MA, Wichman TO (2011) Human health hazards of veterinary medications: information for emergency departments. J Emerg Med 40:198–207. https://doi.org/10.1016/j.jemermed.2009.09.026
2. Shafer SL (2019) Carfentanil: a weapon of mass destruction. Can J Anesth 66:351–355. https://doi.org/10.1007/s12630-019-01295-x
3. Leen JLS, Juurlink DN (2019) Carfentanil: a narrative review of its pharmacology and public health concerns. Can J Anesth 66:414–421. https://doi.org/10.1007/s12630-019-01294-y
4. Haigh JC, Lee LJ, Schweinsburg RE (1983) Immobilization of polar bears with carfentanil. J Wildl Dis 19:140–144. https://doi.org/10.7589/0090-3558-19.2.140
5. Schumacher J, Heard DJ, Young L, Citino SB (1997) Cardiopulmonary effects of carfentanil in dama gazelles (Gazella dama). J Zoo Wildl Med 28:166–170
6. Neumann G, Erhardt W, Oberhuber B, Fritsch R, Blümel G (1980) A new highly potent and short-acting analgesic, carfentanil (R33799), in combination with the hypnotic agent, etomidat (R26490), as a method of anaesthesia in guinea-pigs. Res Exp Med 177:135–143. https://doi.org/10.1007/bf01851842
7. Mutlow A, Isaza R, Carpenter JW, Koch DE, Hunter RP (2004) Pharmacokinetics of carfentanil and naltrexone in domestic goats (*Capra hircus*). J Zoo Wildl Med 35:489–496. https://doi.org/10.1638/03-074
8. Cole A, Mutlow A, Isaza R, Carpenter JW, Koch DE, Hunter RP, Dresser BL (2006) Pharmacokinetics and pharmacodynamics of carfentanil and naltrexone in female common eland (*Taurotragus oryx*). J Zoo Wildl Med 37:318–326. https://doi.org/10.1638/05-070.1
9. Uddayasankar U, Lee C, Oleschuk C, Eschun G, Ariano RE (2018) The pharmacokinetics and pharmacodynamics of carfentanil after recreational exposure: a case report. Pharmacotherapy 38:e41–e45. https://doi.org/10.1002/phar.2117
10. Rabiner EA, Beaver J, Makwana A, Searle G, Long C, Nathan PJ, Newbould RD, Howard J, Miller SR, Bush MA, Hill S, Reiley R, Passchier J, Gunn RN, Matthews PM, Bullmore ET (2011) Pharmacological differentiation of opioid receptor antagonists by molecular and functional imaging of target occupancy and food reward-related brain activation in humans. Mol Psychiatry 16:826–835. https://doi.org/10.1038/mp.2011.29 **(open access article)**
11. Eriksson O, Antoni G (2015) [^{11}C] Carfentanil binds preferentially to μ-opioid receptor subtype 1 compared to subtype 2. Mol Imaging 14:476–483. https://doi.org/10.2310/7290.2015.00019 **(open access article)**
12. Heinz A, Reimold M, Wrase J, Hermann D, Croissant B, Mundle G, Dohmen BM, Braus DH, Schumann G, Machulla HJ, Bares R, Mann K (2005) Correlation of stable elevations in striatal mu-opioid receptor availability in detoxified alcoholic patients with alcohol craving—a positron emission tomography study using carbon 11-labeled carfentanil. Arch Gen Psychiatry 62:57–64. https://doi.org/10.1001/archpsyc.62.1.57
13. Reimold M, Hermann D, Reischl G, Smolka M, Batra A, Rietschel M, Kiefer F, Heinz A, Bares R, Mann K (2010) Reduced mu-opiate receptor availability in a genetic variant of the mu-opiate receptor (A118G): a [^{11}C] carfentanil PET study. J Nucl Med 51(Suppl. 2):49 **(only abstract available)**
14. Weltrowska G, Lemieux C, Chung NN, Guo JJ, Wilkes BC, Schiller PW (2014) 'Carba'-carfentanil (trans isomer): a μ-opioid receptor (MOR) partial agonist with a distinct binding mode. Bioorg Med Chem 22:4581–4586. https://doi.org/10.1016/j.bmc.2014.07.033
15. Riches JR, Read RW, Black RM, Cooper NJ, Timperley CM (2012) Analysis of clothing and urine from Moscow theatre siege casualties reveals carfentanil and remifentanil use. J Anal Toxicol 36:647–656. https://doi.org/10.1093/jat/bks078 **(open access article)**

16. Wax PM, Becker CE, Curry SC (2003) Unexpected "gas" casualties in Moscow: a medical toxicology perspective. Ann Emerg Med 41:700–705. https://doi.org/10.1067/mem.2003.148
17. Tiscione NB, Alford I (2018) Carfentanil in impaired driving cases and the importance of drug seizure data. J Anal Toxicol 42:476–484. https://doi.org/10.1093/jat/bky026 **(open access article)**
18. Misailidi N, Papoutsis I, Nikolaou P, Dona A, Spiliopoulou C, Athanaselis S (2018) Fentanyls continue to replace heroin in the drug arena: the cases of ocfentanil and carfentanil. Forensic Toxicol 36:12–32. https://doi.org/10.1007/s11419-017-0379-4
19. Raffa RB, Pergolizzi JV Jr, LeQuang JA, Taylor R Jr, On behalf of NEMA Research Group, Colucci S, Annabi MH (2018) The fentanyl family: a distinguished medical history tainted by abuse. J Clin Pharm Ther 43:154–158. https://doi.org/10.1111/jcpt.12640 **(open access article)**
20. Elliott SP, Lopez EH (2018) A series of deaths involving carfentanil in the UK and associated post-mortem blood concentrations. J Anal Toxicol 42:e41–e45. https://doi.org/10.1093/jat/bkx109 **(open access article)**
21. Olsson B, Bondesson E, Borgström L, Edsbäcker S, Eirefelt S, Ekelund K, Gustavsson L, Hegelund-Myrbäck T (2011) Pulmonary drug metabolism, clearance, and absorption. In: Smyth HDC, Hickey AJ (eds) Controlled pulmonary drug delivery. Springer, New York
22. Boer F (2003) Drug handling by the lungs. Br J Anaesth 91:50–60. https://doi.org/10.1093/bja/aeg117 **(open access article)**
23. Thum T, Erpenbeck VJ, Moeller J, Hohlfeld JM, Krug N, Borlak J (2006) Expression of xenobiotic metabolizing enzymes in different lung compartments of smokers and nonsmokers. Environ Health Perspect 114:1655–1661. https://doi.org/10.1289/ehp.8861 **(open access article)**
24. Castell JV, Donato MT, Gómez-Lechón MJ (2005) Metabolism and bioactivation of toxicants in the lung. The in vitro cellular approach. Exp Toxicol Pathol 57:189–204. https://doi.org/10.1016/j.etp.2005.05.008
25. Hukkanen J, Pelkonen O, Hakkola J, Raunio H (2002) Expression and regulation of xenobiotic-metabolizing cytochrome P450 (CYP) enzymes in human lung. Crit Rev Toxicol 32:391–411. https://doi.org/10.1080/20024091064273
26. Nhamburo PT, Gonzalez FJ, McBride OW, Gelboin HV, Kimura S (1989) Identification of a new P450 expressed in human lung: complete cDNA sequence, cDNA-directed expression, and chromosome mapping. Biochemistry 28:8060–8066. https://doi.org/10.1021/bi00446a014
27. Feasel MG, Wohlfarth A, Nilles JM, Pang SK, Kristovich RL, Huestis MA (2016) Metabolism of carfentanil, an ultra-potent opioid, in human liver microsomes and human hepatocytes by high-resolution mass spectrometry. AAPS J 18:1489–1499. https://doi.org/10.1208/s12248-016-9963-5
28. Martignoni M, Groothuis GMM, de Kanter R (2006) Species differences between mouse, rat, dog, monkey and human CYP-mediated drug metabolism, inhibition and induction. Expert Opin Drug Metab Toxicol 2:875–894. https://doi.org/10.1517/17425255.2.6.875
29. Hsu F-L, Walz AJ, Myslinski JM, Kong L, Feasel MG, Goralski TDP, Rose T, Cooper NJ, Roughley N, Timperley CM (2019) Synthesis and μ-opioid activity of the primary metabolites of carfentanil. ACS Med Chem Lett 10:1568–1572. https://doi.org/10.1021/acsmedchemlett.9b00404
30. Raunio H, Hakkola J, Hukkanen J, Lassila A, Päivärinta K, Pelkonen O, Anttila S, Piipari R, Boobis A, Edwards RJ (1999) Expression of xenobiotic-metabolizing CYPs in human pulmonary tissue. Exp Toxicol Pathol 51:412–417. https://doi.org/10.1016/s0940-2993(99)80031-1
31. Turpeinen M, Tolonen A, Uusitalo J, Jalonen J, Pelkonen O, Laine K (2005) Effect of clopidogrel and ticlopidine on cytochrome P450 2B6 activity as measured by bupropion hydroxylation. Clin Pharmacol Ther 77:553–559. https://doi.org/10.1016/j.clpt.2005.02.010
32. Walsky RL, Astuccio AV, Obach RS (2006) Evaluation of 227 drugs for in vitro inhibition of cytochrome P450 2B6. J Clin Pharmacol 46:1426–1438. https://doi.org/10.1177/0091270006293753
33. Eagling VA, Tjia JF, Back DJ (1998) Differential selectivity of cytochrome P450 inhibitors against probe substrates in human and rat liver microsomes. Br J Clin Pharmacol 45:107–114. https://doi.org/10.1046/j.1365-2125.1998.00679.x **(open access article)**
34. Ren S, Zeng J, Mei Y, Zhang JZH, Yan SF, Fei J, Chen L (2013) Discovery and characterization of novel, potent, and selective cytochrome P450 2J2 inhibitors. Drug Metab Dispos 41:60–71. https://doi.org/10.1124/dmd.112.048264
35. Patki KC, von Moltke LL, Greenblatt DJ (2003) In vitro metabolism of midazolam, triazolam, nifedipine, and testosterone by human liver microsomes and recombinant cytochromes P450: role of CYP3A4 and CYP3A5. Drug Metab Dispos 31:938–944. https://doi.org/10.1124/dmd.31.7.938
36. Cashman JR, Park SB, Yang ZC, Wrighton SA, Jacob P III, Benowitz NL (1992) Metabolism of nicotine by human liver microsomes: stereoselective formation of trans-nicotine N'-oxide. Chem Res Toxicol 5:639–646. https://doi.org/10.1021/tx00029a008
37. Pelkonen O, Turpeinen M, Uusitalo J, Rautio A, Raunio H (2005) Prediction of drug metabolism and interactions on the basis of in vitro investigations. Basic Clin Pharmacol Toxicol 96:167–175. https://doi.org/10.1111/j.1742-7843.2005.pto960305.x **(open access article)**